A New Measurement of the π^0 Radiative Decay Width

I. Larin,[1,2] D. McNulty,[3] E. Clinton,[4] P. Ambrozewicz,[2] P. Kingsberry,[3,5] D. Lawrence,[6] X. Li,[7] I. Nakagawa,[8] Y. Prok,[3] M. Wood,[4] A. Afanasev,[9] A. Ahmidouch,[2] A. Asratyan,[1] K. Baker,[9] L. Benton,[2] A. Bernstein,[3] P. Cole,[10] P. Collins,[11] D. Dale,[10] S. Danagoulian,[2] G. Davidenko,[1] R. Demirchyan,[2] A. Deur,[6] A. Dolgolenko,[1] G. Dzyubenko,[1] R. Ent,[6] J. Feng,[7] M. Gabrielyan,[8] L. Gan,[7] A. Gasparian,[2,*] S. Gevorkyan,[12] A. Glamazdin,[13] J. Goity,[9] V. Goryachev,[1] V. Gyurjyan,[6] K. Hardy,[2] J. He,[14] M. Ito,[6] L. Jiang,[7] D. Kashy,[6] M. Khandaker,[5] A. Kolarkar,[8] M. Konchatnyi,[13] 0. Korchin,[13] W. Korsch,[8] S. Kowalski,[3] M. Kubantsev,[15] V. Kubarovsky,[6] V. Matveev,[1] B. Mecking,[6] B. Milbrath,[16] R. Minehart,[17] R. Miskimen,[4] V. Mochalov,[18] S. Mtingwa,[2] S. Overby,[2] E. Pasyuk,[11] M. Payen,[2] R Pedroni,[2] B. Ritchie,[11] T. Rodrigues,[19] C. Salgado,[5] A. Shahinyan,[20] A. Sitnikov,[1] D. Sober,[21] S. Stepanyan,[6] W. Stephens,[17] A. Teymurazyan,[8] J. Underwood,[2] A. Vasiliev,[18] B. Volker,[6] V. Vishnyakov,[1] B. Wojtsekowski,[6] and S. Zhou[22]

[1] *Alikhanov Institute for Theoretical and Experimental Physics, Moscow, Russia*
[2] *North Carolina A&T State University, Greensboro, NC 27411, USA*
[3] *Massachusetts Institute of Technology, Cambridge, MA, 02139, USA*
[4] *University of Massachusetts, Amherst, MA, USA*
[5] *Norfolk State University, Norfolk, VA 23504, USA*
[6] *Thomas Jefferson National Accelerator Facility, Newport News, VA 23606, USA*
[7] *University of North Carolina Wilmington, Wilmington, NC 28403, USA*
[8] *University of Kentucky, Lexington, NC 40506, USA*
[9] *Hampton university, Hampton, VA 23606, USA*
[10] *Idaho State University, Pocatello, ID, USA*
[11] *Arizona State University, Tempe, AZ, USA*
[12] *Joint Institute for Nuclear Research, Dubna, 141980, Russia, On leave of absence from Yerevan Physics Institute, Yerevan, Armenia*
[13] *Kharkov Institute of Physics and Technology, Kharkov, Ukraine*
[14] *Institute of High Energy Physics, Chinese Academy of Sciences, Beijing, China*
[15] *Northwestern University, Evanston/Chicago, IL, USA*
[16] *Pacific Northwest National Laboratory, USA*
[17] *University of Virginia, Charlottesville, VA, 22094, USA*
[18] *Institute for High Energy Physics, Protvino, Russia*
[19] *University of São Paulo, São Paulo, Brazil*
[20] *Yerevan Physics Institute, Yerevan, Armenia*
[21] *The Catholic University of America, Washington, DC*
[22] *Chinese Institute of Atomic Energy, Beijing, China*

(Dated: June 27, 2010)

High precision measurements of differential cross sections for π^0 photoproduction at forward angles for two nuclei, ^{12}C and ^{208}Pb, have been performed for incident photon energies of 4.9 - 5.5 GeV to extract the $\pi^0 \to \gamma\gamma$ decay width. The experiment was done at the Jefferson Laboratory using the Hall B photon tagger and a newly developed high resolution multichannel calorimeter. The $\pi^0 \to \gamma\gamma$ decay width was extracted by fitting the measured cross sections with the recently updated theoretical models. Our result is: $\Gamma(\pi^0 \to \gamma\gamma) = 7.82$ eV $\pm$ 1.8% (stat.) $\pm$ 2.1% (syst.)

PACS numbers: 11.80.La, 13.60.Le, 25.20.Lj

The $\pi^0 \to \gamma\gamma$ decay is primarily caused by the chiral anomaly [1, 2], the explicit breaking of a classical symmetry by the quantum fluctuations of the quark fields when they couple to a gauge field, in general, and to the electromagnetic field of photons for this particular case. In the limit of vanishing quark masses (chiral limit) the anomaly prediction is exact, has no adjustable parameters and depends only on a few fundamental parameters: the fine structure constant, the pion decay constant, and the pion mass [1, 2]. Furthermore, in the same chiral limit the $\pi^0 \to \gamma\gamma$ decay width can be calculated exactly to all orders in perturbation theory. However, the current-quark masses are non-vanishing and are approximately $m_u \simeq 4$ MeV and $m_d \simeq 7$ MeV for the light quarks [3, 4]. In addition, there is a strong isospin breaking effect due to the mass difference of the up and down quarks, leading to mixing effects in the light pseudoscalar meson sector. In the past decade several new theoretical calculations of the chiral corrections have been performed based on the framework of chiral perturbation theory (ChPT) [5–7] and QCD sum rules [8]. Due to the small mass of the π^0 meson all higher order theoretical corrections are predicted to be small (the maximum enhancement of the decay width is about 4.8% obtained in [6]) having an estimated uncertainty of less than 1%. The fact that the theory corrections to chiral anomaly are small and they are known with a percent level accuracy makes the $\pi^0 \to \gamma\gamma$ decay channel a benchmark process to test the fundamental predictions of QCD in the energy range of a few GeV.

The current average experimental value for the π^0 decay width given by the PDG [3] is $\Gamma(\pi^0 \to \gamma\gamma) = 7.74 \pm 0.55$ eV. This number is an average of four experiments with much larger dispersion between both the decay width values and their quoted experimental errors, as shown in Fig. 1. The most accurate Primakoff type measurement was done at Cornell by Browman *et al.* [10] with a 5.3% quoted total error: $\Gamma(\pi^0 \to \gamma\gamma) = 7.92 \pm 0.42$ eV. Within the error bar this result agrees with the theory predictions. Two other measurements [11, 12] with relatively large experimental errors ($\simeq 7\%$ and $\simeq 11\%$) differ significantly from each other and do not agree with the theoretical predictions. The most accurate measurement of the π^0 decay width, prior to the current PrimEx experiment, was done by Atherton *et al.* [9] using the direct method of measuring the mean decay length of π^0s produced by a high energy proton beam at CERN. Their result with the quoted 3.1% total error: $\Gamma(\pi^0 \to \gamma\gamma) = 7.25 \pm 0.18 \pm 0.14$ eV is in direct disagreement with the theoretical predictions.

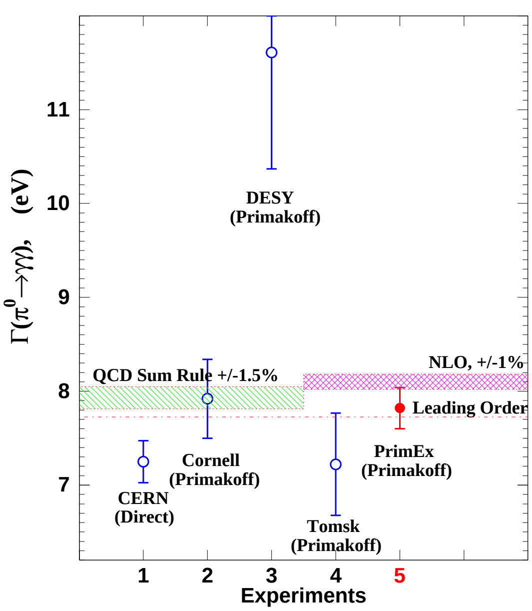

FIG. 1: $\pi^0 \to \gamma\gamma$ decay width in eV. The dashed horizontal line is the LO prediction of the axial anomaly. The r.h.s. shaded band is the NLO chiral perturbation theory prediction [6]. The l.h.s. shaded band is the QCD sum rule prediction [8]. The experimental results, included in the PDG average, are for: (1) the direct method [9]; (2, 3, 4) done with the Primakoff method [10–12]. Also shown (5) is the current PrimEx result.

Clearly, a new Primakoff type of experiment with a precision comparable to, or better than, the direct method measurement [9] was needed to address the experimental situation on this fundamental quantity. With the recent availabilities of high energy, continuous wave (CW), high precision and high intensity photon tagging facilities, together with novel developments in electromagnetic calorimetry, it became feasible to perform high precision cross section measurements of π^0 photoproduction on nuclei at forward directions (the Primakoff method). Combination of these two detection techniques, performed for the first time in these type of experiments, greatly improved not only the angular resolutions, which are critical for Primakoff type of measurements, but significantly reduced all systematic errors dominated in the previous experiments. In addition, to control and verify the precisions in the extracted values, we periodically measured the cross sections of two well known QED processes: Compton scattering and e^+e^- production with the same setup.

The present PrimEx experiment was performed in the fall of 2004 in Hall B of the Jefferson Laboratory (JLab). Incident photons with known timing and energy from the Hall B tagging facility [13] were incident on two 5% *r.l.* targets: ^{12}C and ^{208}Pb [16]. A large acceptance (12.7 mm in diameter) collimator were used to achieve a 1% photon flux uncertainty in the experiment. The relative photon tagging efficiencies were continuously measured during the experiment with the e^+e^- pair spectrometer (PS) consisting of a ~ 1.7 T·m large aperture dipole magnet and two telescopes of scintillating counters located downstream of the physical targets. The absolute normalization of the photon beam to the tagging efficiencies was measured periodically by a total absorption counter (TAC) at low beam intensities. The decay photons from $\pi^0 \to \gamma\gamma$ were detected in the multichannel Hybrid electromagnetic Calorimeter (HyCal) located at 7.5 m downstream from the physical targets to provide a large geometrical acceptance ($\sim 70\%$). The HyCal calorimeter consists of 1152 $PbWO_4$ crystal shower detectors ($2.05 \times 2.05 \times 18.0$ cm^3) in the central part surrounded by 576 lead glass Cherenkov counters ($3.82 \times 3.82 \times 45.0$ cm^3). Four crystal detectors are removed from the central part of the calorimeter (4.1×4.1 cm^2 hole in size) for passage of the high intensity ($\sim 10^7$ γ/s) incident photon beam through the calorimeter [14]. Eleven 5 mm thick scintillator counters, located in front of HyCal, provided rejection of charged particles and effectively reduced the background in the experiment. To minimize the decay photon conversion in air, the distance from the PS magnet to HyCal was covered by a helium bag at atmospheric pressure. The photon beam position stability during the experiment was controlled by an X,Y-scintillator fiber detector, located downstream from HyCal [15].

Coincidences between the photon tagger in the upper energy interval (4.9 - 5.5 GeV) and the HyCal calorimeter with a total deposited energy greater than 2.5 GeV gave the experimental trigger. The combination of the photon tagger and the calorimeter defined the following major event selection criteria in this experiment: (1) timing between the incident photon and decay photons in the calorimeter ($\sigma_t = 1.1$ ns); (2) energy difference between tagger and total energy in the calorimeter (elasticity, ignoring the recoil energy of the nuclei, shown in Fig. 2 for one angular bin); (3) invariant mass of two photons in the calorimeter (Fig. 3).

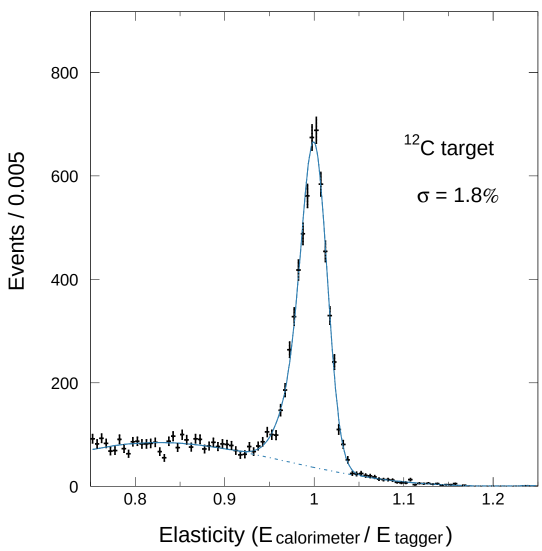

FIG. 2: Distribution of reconstructed elasticity.

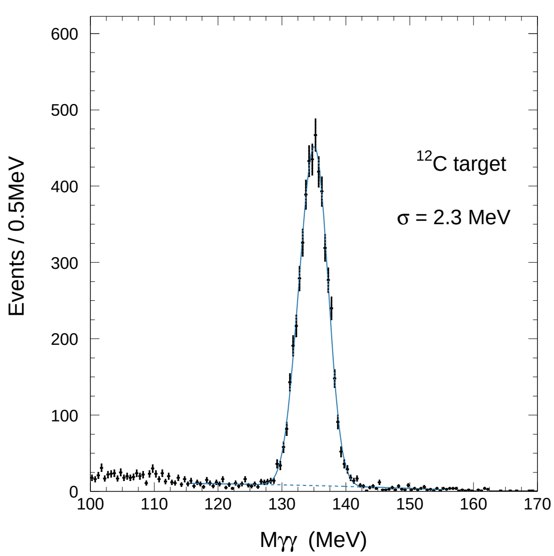

FIG. 3: Distribution of reconstructed invariant mass.

The event yield (the number of π^0 events for each production angle bin) was obtained from the data by applying the selection criteria, mentioned above, and fitting the experimental distributions for each angular bin. As illustrated in Fig. 2 and Fig. 3, the typical background in the event selection process was only a few percent of the real signal events. However, the uncertainty in the background extraction in this much upgraded experiment still remains as one of the largest contributions to the systematic error budget shown in Table II.

The extraction of differential cross sections from the experimental yields requires an accurate knowledge of the total photon flux for each tagger energy bin, the number of atoms in the target, the acceptance of the experimental setup and the inefficiencies of the detectors. The photon flux in this experiment was measured by the tagger (calibrated by the TAC) and was monitored on-line by the PS. The uncertainty reached on this important parameter was at the level of 1% ([15]). Different techniques have been used to determine the number of atoms in both the targets with an uncertainty better than 0.1% [16]. The acceptance and errors on the detection efficiencies were simulated by a GEANT-based Monte Carlo code that included accurate information about the detector geometry and responses from each detector element [15]. Other than accidental backgrounds, some physics processes with an energetic π^0 in the final state can potentially contribute to the extracted yield. It was shown that the only sizable contribution comes from the ω photoproduction process through the $\omega \rightarrow \pi^0\gamma$ decay channel. The fit of the experimental data, as described below, with the subtracted physics background changes the extracted π^0 decay width by 1.4% with an uncertainty of 0.25% (included in Table II).

The resulting experimental cross sections for ^{12}C and ^{208}Pb are shown in Fig. 4 and Fig. 5 along with the fit results for individual contributions from the different π^0 production mechanisms. Two elementary amplitudes, the Primakoff (one photon exchange) T_P, and the strong (hadron exchange) T_S, contribute coherently, as well as incoherently in the π^0 photoproduction process on nuclei at forward angles. The cross section of this process can be expressed by four terms: Primakoff (Pr), Nuclear Coherent (NC), Interference (Int), and Nuclear Incoherent (NI):

$$\begin{aligned}\frac{d\sigma}{d\Omega} &= \mid T_{Pr} + e^{i\varphi} T_S \mid^2 + \frac{d\sigma_{NI}}{d\Omega} \\ &= \frac{d\sigma_{Pr}}{d\Omega} + \frac{d\sigma_{NC}}{d\Omega} + \frac{d\sigma_{Int}}{d\Omega} + \frac{d\sigma_{NI}}{d\Omega},\end{aligned}$$

where φ is the relative phase between the Primakoff and the strong amplitudes. The Primakoff cross section is proportional to the π^0 decay width, the primary focus of this experiment [10]:

$$\frac{d\sigma_{Pr}}{d\Omega} = \Gamma(\pi^0 \rightarrow \gamma\gamma)\frac{8\alpha Z^2}{m^3}\frac{\beta^3 E^4}{Q^4}|F_{e.m.}(Q)|^2 \sin^2\theta_\pi,$$

where Z is the atomic number; m, β, θ_π are the mass, velocity and production angle of the pion; E is the energy of incident photon; Q is the four-momentum transfer to the nucleus; $F_{e.m.}(Q)$ is the nuclear electromagnetic form factor, corrected for final state interactions (FSI) of the outgoing pion. The FSI effects of the photoproduced π^0s, as well as the photon shadowing effect in nuclear matter, need to be accurately included in the cross section calculations to provide a percent level extraction of the Primakoff amplitude, and therefore, the decay width. To achieve this, and to calculate the NC and NI cross sections, a full theoretical description based on the Glauber method was developed, providing an accurate calculation of those processes in both light and heavy nuclei [17, 18]. For the nuclear incoherent process, an independent method based on the multi-collision intranuclear cascade model [19] was also used to double check the model dependence of the extracted decay width (see Table II).

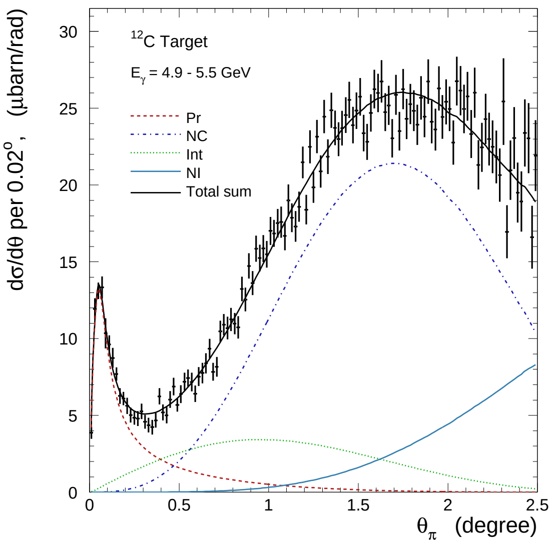

FIG. 4: Differential cross section as a function of π^0 production angle for ^{12}C. Contribution of different processes, obtained from the fit, are shown with lines (see the text).

The $\Gamma(\pi^0 \to \gamma\gamma)$ decay width was extracted by fitting the experimental results with the theoretical cross sections of the four processes mentioned above folded with the angular resolutions and the measured energy spectrum of the incident photons. In the fitting process, four parameters: $\Gamma(\pi^0 \to \gamma\gamma)$, C_{NC}, C_{NI}, φ were kept free to vary the magnitude of the Primakoff, NC, NI cross sections and the phase angle, respectively. Several groups independently analyzed the experimental data. The weighted average results from these groups are presented in Table I for ^{12}C and ^{208}Pb.

Our result combined for the two targets is $\Gamma(\pi^0 \to \gamma\gamma) = 7.82$ eV $\pm$ 1.8% (stat.) $\pm$ 2.1% (syst.). The quoted total systematic error is the quadratic sum of all estimated errors listed in Table II. The

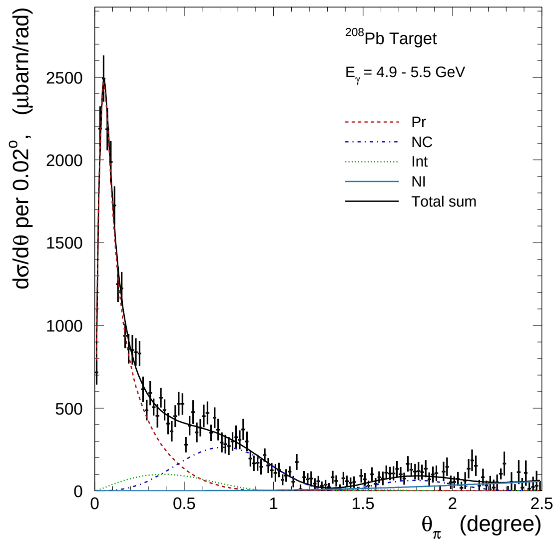

FIG. 5: Differential cross section as a function of π^0 production angle for ^{208}Pb. Contribution of different processes, obtained from the fit, are shown with lines (see the text).

Target	$\Gamma(\pi^0\to\gamma\gamma)$ [eV]	C_{NC}	φ [rad]	C_{NI}	$\frac{\chi^2}{N_{df}}$
^{12}C	7.79±0.18	0.83±0.02	0.78±0.07	0.72±0.06	$\frac{152}{121}$
^{208}Pb	7.85±0.23	0.69±0.04	1.25±0.07	0.68±0.12	$\frac{123}{121}$

TABLE I: The fit values extracted from the measured cross sections on ^{12}C and ^{208}Pb targets. The errors shown here are statistical only (see the text for notations).

systematic errors in this experiment were verified by measuring the cross sections of the Compton scattering and the e^+e^- production processes. The extracted cross sections for these well known processes agree with the theory predictions at the level of 1.5% and will be published separately. Our result, with the 2.8% total experimental error, is the most precise measurement of the $\Gamma(\pi^0 \to \gamma\gamma)$ to date. It is a factor of two-and-a-half times more accurate than the current knowledge (as quoted in the PDG) on this important fundamental quantity. As a single experimental result, it directly confirms the validity of the chiral anomaly in QCD. To check the effects of chiral corrections to the anomaly, a factor of two more precise measurement is required. The second stage of this experiment is currently planned to run at JLab within the next few years to reach the projected 1.4% precision.

We thank the JLab physics and accelerator divisions for their contributions. We extend our special thanks to Hall B engineering group for their critical contributions in setup design, construction and installation stages of this experiment. This experimental project was supported in

photon flux	1.0%
target thickness (atoms/cm^2)	0.1%
event selection	1.6%
HyCal efficiency	0.5%
beam energy and parameters	0.4%
veto efficiency	0.4%
geometrical acceptance	0.3%
model dependence	0.3%
physics background	0.25%
trigger efficiency	0.1%
branching ratio	0.03%
Total	2.1%

TABLE II: Estimated systematic errors

part by the National Science Foundation under a Major Research Instrumentation (MRI) grant (PHY-0079840).

---

* Corresponding author:gasparan@jlab.org

[1] J.S. Bell and R. Jackiw, Nuovo Cimento **60A**, 47 (1969).
[2] S.L. Adler, Phys. Rev. **177**, 2426 (1969).
[3] C. Amsler *et al.*, (Particle Data Group), Phys. Lett. **B667**, 1 (2008).
[4] H. Leutwyler, Phys. Lett. **B378**, 313 (1996).
[5] B. Moussallam, Phys. Rev. **D51**, 4939 (1995).
[6] J. Goity, A. Bernstein, B. Holstein, Phys. Rev. **D66**, 076014 (2002).
[7] B. Ananthanarayan, B. Moussallam, JHEP **05**, 052 (2002).
[8] B.L. Ioffe, A.G. Oganesian, Phys. Lett. **B647**, 389 (2007).
[9] H.W. Atherton *et al.*, Phys. Lett. **B158**, 81 (1985).
[10] A. Browman *et al.*, Phys. Rev. Lett. **33**, 1400 (1974).
[11] G. Bellettini *et al.*, Nuovo Cimento **66A**, 243 (1970).
[12] V.I. Kryshkin *et al.*, Sov. Phys. JETP, vol. 30, no. 6, 1037 (1970).
[13] D.I. Sober *et al.*, Nucl. Instr. and Meth. **A440/2**, 263 (2000).
[14] A. Gasparian, *Calorimetry in Particle Physics*, World Scientific, 109-115 (2004).
[15] http://www.jlab.org/primex/.
[16] P. Martel *et al.*, Nucl. Instr. and Meth. **A612**, 46 (2009).
[17] S. Gevorkyan *et al.*, Phys. Rev. **C80**, 055201 (2009).
[18] S. Gevorkyan *et al.*, hep-ph arXiv: 0908.1297, submitted to Phys. Rev. C.
[19] T.E. Rodrigues *et al.*, Phys. Rev. **C71**, 051603 (2005).